Advances in Aircraft and Spacecraft Science, *Vol. 7, No. 4 (2020) 335-351*
DOI: https://doi.org/10.12989/aas.2020.7.4.335

Thermal buckling analysis of functionally graded sandwich cylindrical shells

Ahmed Amine Daikh*[1,2]

[1]*Structural Engineering and Mechanics of Materials Laboratory, Department of Civil Engineering, Mascara, Algeria*
[2]*Mechanics of Structures and Solids Laboratory, Faculty of Technology, University of Sidi Bel Abbes, Algeria*

(Received July 11, 2019, Revised May 5, 2020, Accepted May 12, 2020)

Abstract. Thermal buckling of functionally graded sandwich cylindrical shells is presented in this study. Material properties and thermal expansion coefficient of FGM layers are assumed to vary continuously through the thickness according to a sigmoid function and simple power-law distribution in terms of the volume fractions of the constituents. Equilibrium and stability equations of FGM sandwich cylindrical shells with simply supported boundary conditions are derived according to the Donnell theory. The influences of cylindrical shell geometry and the gradient index on the critical buckling temperature of several kinds of FGM sandwich cylindrical shells are investigated. The thermal loads are assumed to be uniform, linear and nonlinear distribution across the thickness direction. An exact simple form of nonlinear temperature rise through its thickness taking into account the thermal conductivity and the inhomogeneity parameter is presented.

Keywords: FGM sandwich cylindrical shells; thermal buckling; nonlinear temperature rise; Donnell theory

1. Introduction

Functionally Graded Materials (FGM) are a novel class of composite materials. Whereas traditional composites are homogeneous in composition, FGMs possess a gradual spatial compositional variation of the composite material in terms of volume fraction and microstructure (Miyamoto *et al.* 1999). These new materials were proposed to reduce the local stress concentrations induced by abrupt transitions in material properties across the interface between discrete materials (Finot *et al.* 1996). FGMs were first suggested for thermal barrier coatings in aerospace structural applications and fusion reactors. They are now developed for general use in various fields of engineering. Typically, FGMs are made of a ceramic and a metal for the purpose of thermal protection against large temperature gradients. The ceramic material has excellent characteristics in heat resistance due to its low thermal conductivity. On the other hand, the ductile metal constituent prevents fracture due to its greater toughness. Functionally graded structures can be seen in nature. For example, the bone, human skin and the bamboo tree are all different forms of FGM.

Circular FGM cylindrical shell is a common structure in many engineering fields like nuclear

*Corresponding author, Ph.D., E-mail: daikh.ahmed.amine@gmail.com

http://www.techno-press.org/?journal=aas&subpage=7 ISSN: 2287-528X (Print), 2287-5271 (Online)

reactor, gun barrel, aerospace component, and heat supply pipeline. Due to the importance and wide engineering applications of composites, a number of investigations dealing with thermal buckling of circular cylindrical shell had been published in the scientific literature. Thangaratnam et al (1990) used the finite element method (FEM) to examine the linear buckling analysis of laminated composite conical and cylindrical shells subjected to thermal loadings. Based on the first-order shell theory Shahsiah and Eslami (2003a, b) analyzed the thermal buckling of a functionally graded cylindrical shell by using the Sanders kinematic relations, and the Donnell stability equations. Three types of thermal loading as uniform temperature rise, linear and nonlinear temperature rise through-the-thickness were considered. The effect of imperfections on thermal buckling of functionally graded cylindrical shells for two different models of initial imperfections has been given by Mirzavand and Eslami (2005, 2006). They have also analyzed thermal buckling of simply supported FGM cylindrical shells that are integrated with surface-bonded piezoelectric actuators using the third-order shear deformation shell theory and different types of thermal loads (Mirzavand and Eslami 2007). Wu *et al.* (2005) proposed closed form solutions for the critical buckling temperature differences of shells by using the classical shell theory. Kadoli and Ganesan (2006) analyzed of temperature-dependent clamped-clamped FGM cylinders using the FSDT. Based on the first-order shear deformation shell theory, Sheng and Wang (2008) studied thermal vibration, buckling and dynamic instability of FGM cylindrical shells embedded in an elastic medium, subjected to mechanical and thermal loads. The influence of geometrical imperfections on thermal instability of FG cylindrical shells using Donnell stability equations and Wan-Donnell model for axisymmetric imperfection is analyzed by Hoang and Nguyen (2008). On the basis of first order shear deformation theory (FSDT), Sheng and Wang (2008) studied dynamic stability, vibration and buckling of FGM cylinders under thermal and static axial loading. Najafizadeh *et al.* (2009) studied the influence of axial compression loads on static of FGM cylindrical shells stiffened by stringers and rings. The same authors (Sheng and Wang 2010) examined the buckling of FGM cylindrical shells by taking into account the piezoelectric and thermal loads effect. The effect of pure bending loading on the buckling response of FGM cylinders is investigated by Huang *et al.* (2011). Bagherizadeh *et al.* (2012) carried out thermal buckling behavior of cylindrical shells made of FGM in contact with the Pasternak elastic foundation subjected to uniform temperature rise based on the third-order shear deformations shell theory. A theoretical analysis on buckling and vibration characteristic of FGM magneto-electro-thermo-elastic circular cylindrical shell are carried out by Zhang and Li (2013). By using the higher order shear deformation theory (HSDT), Lang and Xuewu (2013) investigated the effect of external loads, temperature, surface electric voltage and magnetic voltage, on the buckling behavior of FGM magneto-electro-thermo-elastic cylinders. The effect of the thickness variability and bidirectional material heterogeneity on the thermal buckling of cylindrical shells is investigated by Shariyat and Asgari (2013) by employing the third order shear deformation theory (TSDT), von Karman-type kinematic nonlinearity, and a nonlinear finite element method. Dung and Nga (2013) employed an analytical approach to analyze the effect of mechanical compressive loads and external pressures on the buckling and post-buckling behavior of an eccentrically stiffened FGM cylindrical shell. Based on the Donnell theory of shells combined with the von Kármán type of geometrical nonlinearity, thermal buckling of FGM cylindrical shells in two-parameter elastic foundation with regard to temperature dependency of the constituents has been given by Sabzikar *et al.* (2014). Based on the FSDT, Sofiyev (2014) studied static and dynamic of four types of sandwich cylindrical shells covered by different coatings subjected to the hydrostatic pressure. Zhang *et al.* (2015) used classical shell theory to examined buckling responses of

elastoplastic FGM cylindrical shells subjected to axial compression and external pressure. Asadi *et al.* (2015) investigated the thermal instability of geometrically imperfect sandwich cylindrical shells made of a shape memory alloy (SMA)-fiber-reinforced composite and functionally graded face sheets based on the TSDT, von Karman geometrical nonlinearity and initial imperfection. Post-buckling response of FGM cylinders with spiral stiffeners using the classical plate theory (CPT) resting on elastic foundation is investigated by Shaterzadeh and Foroutan (2016). The static response of temperature-dependent and temperature-independent curved cylindrical, spherical, elliptical and hyperbolic shell panels is examined by Kar *et al.* (2016) on the basis of using finite element steps. Thang *et al.* (2016) examined buckling of sigmoid FGM cylindrical panels by considering the influences of variable thickness and imperfection. They have also analyzed FGM cylinders reinforced by stringers subjected to thermal and torsional loads (Thang *et al.* 2016). Sun *et al.* (2016) employed a new analytical method for buckling of FGM and carbon nanotubes (CNTs) cylindrical nano-shells under to compressive and thermal loads. Mehralian *et al.* (2016) examined buckling of FGM piezoelectric cylindrical nano-shell using a novel modified couple stress theory. Nasirmanesh and Mohammadi (2016) utilized the finite element method to studied buckling response of cracked FGM cylindrical shells under different loading conditions. Wan and Li (2017) used the classical Donnell shell theory to analyze thermal buckling of simply supported and clamped FGM cylindrical shell. Ni *et al.* (2017) employed Hamiltonian-based approach to study the vibration of functionally graded orthotropic circular cylindrical shell embedded in an elastic medium. Han *et al.* (2017) developed numerical approach for buckling behavior the cylindrical shell with FGM coating under thermal loads. Using the Reissner's shell theory, Ni *et al.* (2018) investigated thermal buckling of FGM orthotropic cylindrical shells with temperature-dependent material properties. Zhou *et al.* (2019a) studied nonlinear static response of functionally graded porous graphene platelet reinforced composite cylindrical shells using Donnell's theory and the HSDT. They have also investigated the effect of combined loads on the stability of functionally graded multilayer hybrid composite cylindrical shells by employing a novel two-steps micromechanical model for hybrid composites (Zhou *et al.* 2019b). Trabelsi *et al.* (2019) analyzed the response of thermal buckling of functionally graded plates and cylindrical shells by utilizing modified FSDT-based four nodes finite shell element.

With the developments in manufacturing methods, the FGMs are taken into account in the sandwich structure industries. In general, the sudden change in the material properties of sandwich structure from one layer to another can result in stress concentrations which often lead to delamination. To overcome this problem, The FG sandwich structure is proposed because of the gradual variation of material properties at the interfaces between the face layers and the core.

Generally, material properties of FGM sandwich layers are varying continuously through-the-thickness according to power-law FGM (P-FGM). The FGM sandwich structure can alleviate the large interfacial shear stress concentration at the interfaces between the face sheets and the core. The use of sigmoid FGM sandwiches (S-FGM) can reduce these stresses more.

In the present article, thermal buckling of simply supported P-FGM and S-FGM sandwich cylindrical shells is studied. A simple form of nonlinear temperature rise through its thickness taking into account the thermal conductivity and the inhomogeneity parameter is presented. The material properties such as the coefficient of thermal expansion and Young's modulus are varied continuously through the thickness according to a sigmoid and power-law function. The equilibrium equations of functionally graded cylindrical shell are derived according to the Donnell's theory.

2. Functionally graded sandwich cylindrical shells

Consider a functionally graded sandwich cylindrical shell made of three layers of arbitrary thickness h, mid-surface radius R and length L as shown in Fig. 1. We use cylindrical coordinates with the origin located at the mid-surface of the cylinder, and coordinates x, θ, and z in the axial, the circumferential, and the thickness directions, respectively. The inner and outer faces of the cylindrical shell are at $z = \pm h/2$. The thicknesses positions of the inner, the two interfaces, and the outer layers are denoted by $h_0 = -h/2,\ h_1,\ h_2,\ h_3 = h/2$, respectively (Fig. 2). The face layers are graded from metal to ceramic while the core layer is made of ceramic. Two Types of sandwich cylindrical shells are used: a sandwich cylindrical shell with simple power-law functionally graded face layers (P-FGM) and a sandwich cylindrical shell with sigmoid functionally graded face layers (S-FGM).

2.1 Sandwich cylindrical shell with power-law functionally graded face layers

The sandwich cylindrical shell is composed of three layers, two functionally graded face layers based on power-law function (P-FGM) and homogeneous core layer. The inner and the outer layers are graded from metal to ceramic, while the core layer is made of ceramic. The volume fraction of the P-FGM sandwich cylindrical shell varies through-the-thickness as follows (Zenkour and Sobhy 2010)

$$\begin{aligned} V^{(1)}(z) &= \left(\frac{z-h_0}{h_1-h_0}\right)^k, \qquad h_0 \le z \le h_1 \\ V^{(2)}(z) &= 1, \qquad h_1 \le z \le h_2 \\ V^{(3)}(z) &= \left(\frac{z-h_3}{h_2-h_3}\right)^k, \qquad h_2 \le z \le h_3 \end{aligned} \tag{1}$$

where k denotes volume fraction index, which takes values greater than or equal to zero.

2.1 Sandwich cylindrical shell with sigmoid functionally graded face layers

In this type of sandwich cylinders, the face layers are made of sigmoid functionally graded material (S-FGM). The volume fraction of the S-FGM sandwich shell varies through-the-thickness as follows (Daikh and Zenkour 2019 a, b)

$$\begin{aligned} V_1^{(1)}(z) &= \frac{1}{2}\left(\frac{z-h_0}{h_m-h_0}\right)^k, \qquad h_0 \le z \le h_m \\ V_2^{(1)}(z) &= 1-\frac{1}{2}\left(\frac{z-h_1}{h_m-h_1}\right)^k, \qquad h_m \le z \le h_1 \\ V^{(2)}(z) &= 1, \qquad h_1 \le z \le h_2 \\ V_1^{(3)}(z) &= 1-\frac{1}{2}\left(\frac{z-h_2}{h_n-h_2}\right)^k, \qquad h_2 \le z \le h_n \\ V_2^{(3)}(z) &= \frac{1}{2}\left(\frac{z-h_3}{h_n-h_3}\right)^k, \qquad h_n \le z \le h_3 \end{aligned} \tag{2}$$

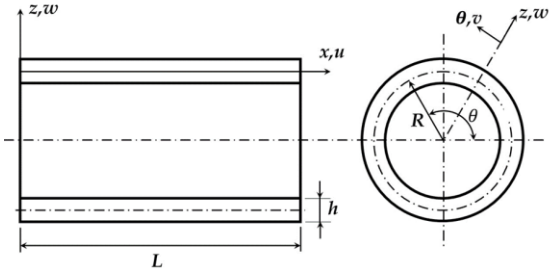

Fig. 1 Configuration and coordinate system of cylindrical shell

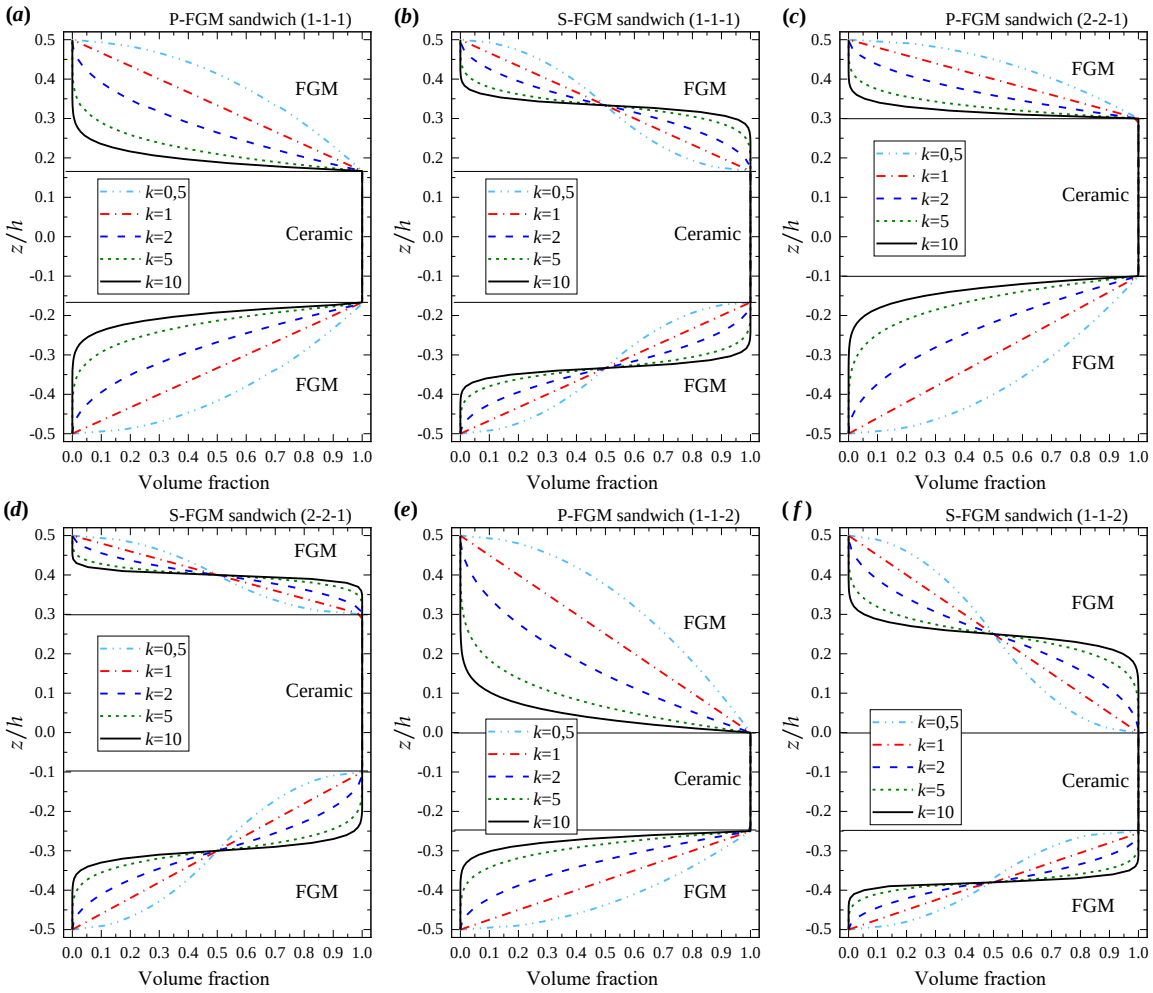

Fig. 2 Variation of volume fraction through-the-thickness of FGM sandwich cylindrical shell

where $h_m = (h_1 + h_2)/2$ and $h_n = (h_2 + h_3)/2$ denotes the middle surface positions of the inner layer and the outer layer, respectively.

By using the rule of mixture, the material properties of each layer n (n=1, 2, 3), like the modulus of elasticity E, the coefficient of thermal conductivity K and the coefficient of thermal expansion α, can be expressed as

$$P^{(n)}(z) = V^{(n)}(z).P_m + \left[1 - V^{(n)}(z)\right].P_c \tag{3}$$

where P_m and P_c are the corresponding properties of the metal and ceramic, respectively.

3. Mathematical formulation

Consider a sandwich cylindrical shell of mean radius R and thickness h with length L (Fig. 1). The normal and shear strains at distance z from the shell middle surface based on the Donnell shell theory are (Brush and Almroth 1975)

$$\varepsilon_x = \varepsilon_x^0 + z\kappa_x,\ \varepsilon_\theta = \varepsilon_\theta^0 + z\kappa_\theta,\ \gamma_{x\theta} = \gamma_{x\theta}^0 + z \tag{4}$$

where

$$\varepsilon_x^0 = \frac{\partial u}{\partial x} + \frac{1}{2}\frac{\partial w^2}{\partial x},\ \varepsilon_\theta^0 = \frac{1}{R}\left(\frac{\partial v}{\partial \theta} + w\right) + \frac{1}{2R^2}\left(v - \frac{\partial w}{\partial \theta}\right)^2,$$
$$\gamma_{x\theta}^0 = \frac{\partial v}{\partial x} + \frac{1}{R}\frac{\partial u}{\partial \theta} + \frac{1}{R}\frac{\partial w}{\partial x}\left(\frac{\partial w}{\partial \theta} - v\right), \tag{5}$$
$$\kappa_x = -\frac{\partial^2 w}{\partial x^2},\quad \kappa_\theta = -\frac{1}{R^2}\frac{\partial^2 w}{\partial \theta^2},\quad \kappa_{x\theta} = -\frac{1}{R}\frac{\partial^2 w}{\partial x \partial \theta}$$

where u, v, and w denote the axial, circumferential, and lateral displacements of the cylindrical shell, respectively. The constitutive relations of the sandwich cylindrical shell can be written as

$$\begin{Bmatrix} \sigma_x \\ \theta_\theta \\ \tau_{x\theta} \end{Bmatrix}^n = \begin{bmatrix} Q_{11} & Q_{12} & 0 \\ Q_{21} & Q_{22} & 0 \\ 0 & 0 & Q_{66} \end{bmatrix}^n \begin{Bmatrix} \varepsilon_x - \alpha(\mathrm{z})^n \mathrm{T} \\ \varepsilon_\theta - \alpha(\mathrm{z})^n \mathrm{T} \\ \gamma_{x\theta} \end{Bmatrix} \tag{6}$$

where

$$Q_{11}^{(n)} = Q_{22}^{(n)} = \frac{E^{(n)}(z)}{1-\upsilon^2},\ Q_{12}^{(n)} = \upsilon Q_{11}^{(n)},\ Q_{66}^{(n)} = \frac{E^{(n)}(z)}{2(1+\upsilon)} \tag{7}$$

and $T(x, y, z)$ is the temperature rise through the thickness.

The force and moment resultants may be presented as

$$\begin{Bmatrix} N_x \\ N_\theta \\ N_{x\theta} \end{Bmatrix} = \sum_{n=1}^{3} \int_{h_{n-1}}^{h_n} \begin{Bmatrix} \sigma_x \\ \sigma_y \\ \tau_{x\theta} \end{Bmatrix}^{(n)} \mathrm{d}z,\ \begin{Bmatrix} M_x \\ M_\theta \\ M_{x\theta} \end{Bmatrix} = \sum_{n=1}^{3} \int_{h_{n-1}}^{h_n} \begin{Bmatrix} \sigma_x \\ \sigma_\theta \\ \tau_{x\theta} \end{Bmatrix}^{(n)} z\mathrm{d}z \tag{8}$$

The stress resultants of a sandwich cylindrical shell are related to the strains by the relations

$$\begin{Bmatrix} N_x \\ N_\theta \\ N_{x\theta} \\ M_x \\ M_\theta \\ M_{x\theta} \end{Bmatrix} = \begin{bmatrix} A_{11} & A_{12} & 0 & B_{11} & B_{12} & 0 \\ A_{21} & A_{22} & 0 & B_{12} & B_{22} & 0 \\ 0 & 0 & D_{11} & 0 & 0 & D_{22} \\ B_{11} & B_{12} & 0 & D_{11} & D_{12} & 0 \\ B_{21} & B_{22} & 0 & D_{12} & D_{22} & 0 \\ 0 & 0 & D_{22} & 0 & 0 & D_{66} \end{bmatrix} \begin{Bmatrix} \varepsilon_x^0 \\ \varepsilon_\theta^0 \\ \gamma_{x\theta}^0 \\ k_x \\ k_\theta \\ k_{x\theta} \end{Bmatrix} - \begin{Bmatrix} N_T \\ N_T \\ 0 \\ M_T \\ M_T \\ 0 \end{Bmatrix} \tag{9}$$

where

$$\{A_{ij}, B_{ij}, D_{ij}\} = \sum_{n=1}^{3} \int_{h_{n-1}}^{h_n} Q_{ij}{}^{(n)}\{1, z, z^2\}dz\,, (i, j = 1,2,6) \tag{10}$$

and $\{N^T\}, \{M^T\}$ are the thermal force

$$\{N_T, M_T\} = \sum_{n=1}^{3} \int_{h_{n-1}}^{h_n} \{\beta\}^{(n)} T\{1, z\}\mathrm{d}z \tag{11}$$

where

$$\{\beta\}^{(n)} = \begin{Bmatrix} (Q_{11} + Q_{12})\alpha \\ (Q_{12} + Q_{22})\alpha \\ 0 \end{Bmatrix}^{(n)} \tag{12}$$

4. Stability equations

By using Donnell shell theory, the equilibrium equations for general thin cylindrical shell are obtained as

$$\begin{gathered} \frac{\partial N_x}{\partial x} + \frac{1}{R}\frac{\partial N_{x\theta}}{\partial \theta} = 0 \quad \frac{1}{R}\frac{\partial N_\theta}{\partial \theta} + \frac{\partial N_{x\theta}}{\partial x} = 0 \\ \frac{\partial^2 M_x}{\partial x^2} + \frac{2}{R}\frac{\partial^2 M_{x\theta}}{\partial x \partial \theta} + \frac{1}{R^2}\frac{\partial^2 M_\theta}{\partial \theta^2} - \frac{1}{R}N_\theta + \bar{N}_x^0 \frac{\partial^2 w}{\partial x^2} + \bar{N}_\theta^0 \frac{\partial^2 w}{\partial \theta^2} + \frac{2}{R}\bar{N}_{x\theta}^0 \frac{\partial^2 w}{\partial x \partial \theta} = 0 \end{gathered} \tag{13}$$

Assuming that the equilibrium state of the cylindrical shell under thermal loads may be designated by $u^0,\ v^0,\ w^0$. The displacement components of a neighboring stable state differ by $u^1,\ v^1,\ w^1$ with respect to the equilibrium position. The displacements of a neighboring state are

$$u = u^0 + u^1, \qquad v = v^0 + v^1, \qquad w = w^0 + w^1 \tag{14}$$

where the terms with subscripts 0 refers to the state of equilibrium conditions and the terms with subscripts 1 refers to the state of stability. Note that whereas the equilibrium equations are nonlinear, the stability equations are linear.

The linearized strains and curvatures in terms of the displacement component are

$$\begin{gathered} \varepsilon_x^{0\,1} = \frac{\partial u^1}{\partial x}, \qquad \varepsilon_\theta^{0\,1} = \frac{1}{R}\left(\frac{\partial v^1}{\partial \theta} + w^1\right), \qquad \gamma_{x\theta}^{0\ \ 1} = \frac{\partial v^1}{\partial x} + \frac{1}{R}\frac{\partial u^1}{\partial \theta}, \\ \kappa_x{}^1 = -\frac{\partial^2 w^1}{\partial x^2}, \qquad \kappa_\theta{}^1 = -\frac{1}{R^2}\frac{\partial^2 w^1}{\partial \theta^2}, \qquad \kappa_{x\theta}{}^1 = -\frac{1}{R}\frac{\partial^2 w^1}{\partial x \partial \theta} \end{gathered} \tag{15}$$

The stress and moment resultants may be related to the equilibrium and neighboring states as

$$\begin{gathered} N_x = N_x^0 + N_x^1, \qquad N_\theta = N_\theta^0 + N_\theta^1, \qquad N_{x\theta} = N_{x\theta}^0 + N_{x\theta}^1 \\ M_x = M_x^0 + M_x^1, \qquad M_\theta = M_\theta^0 + M_\theta^1, \qquad M_{x\theta} = M_{x\theta}^0 + M_{x\theta}^1 \end{gathered} \tag{16}$$

Eliminating the pre-buckling equilibrium expressions and ignoring the nonlinear terms of the incremental variables, we obtain the governing equations for buckling according to the Donnell theory as follows

$$\frac{\partial N_x^1}{\partial x}+\frac{1}{R}\frac{\partial N_{x\theta}^1}{\partial \theta}=0 \quad \frac{1}{R}\frac{\partial N_\theta^1}{\partial \theta}+\frac{\partial N_{x\theta}^1}{\partial x}=0$$
$$\frac{\partial^2 M_x^1}{\partial x^2}+\frac{2}{R}\frac{\partial^2 M_{x\theta}^1}{\partial x\partial \theta}+\frac{1}{R^2}\frac{\partial^2 M_\theta^1}{\partial \theta^2}-\frac{1}{R}N_\theta^1+\bar{N}_x^0\frac{\partial^2 w^1}{\partial x^2}+\bar{N}_\theta^0\frac{\partial^2 w^1}{\partial \theta^2}+\frac{2}{R}\bar{N}_{x\theta}^0\frac{\partial^2 w^1}{\partial x\partial \theta}=0 \tag{17}$$

where

$$\bar{N}_x^0=-N_T, \text{ and } \bar{N}_\theta^0=\bar{N}_{x\theta}^0=0 \tag{18}$$

The forces and moments associated with the stability state are

$$N_x^1=A_{11}\frac{\partial u^1}{\partial x}+A_{12}\left(\frac{w^1}{R}+\frac{\partial v^1}{R\partial \theta}\right)-B_{11}\frac{\partial^2 w^1}{\partial x^2}-B_{12}\frac{\partial^2 w^1}{R^2\partial \theta^2}$$
$$N_\theta^1=A_{12}\frac{\partial u^1}{\partial x}+A_{22}\left(\frac{w^1}{R}+\frac{\partial v^1}{R\partial \theta}\right)-B_{22}\frac{\partial^2 w^1}{R^2\partial \theta^2}-B_{12}\frac{\partial^2 w^1}{\partial x^2}$$
$$N_{x\theta}^1=A_{66}\left(\frac{\partial v^1}{\partial x}+\frac{\partial u^1}{R\partial \theta}\right)-B_{66}\frac{\partial^2 w^1}{R\partial x\partial \theta}$$
$$M_x^1=B\frac{\partial u^1}{\partial x}+B_{12}\left(\frac{w^1}{R}+\frac{\partial v^1}{R\partial \theta}\right)-D_{11}\frac{\partial^2 w^1}{\partial x^2}-D_{12}\frac{\partial^2 w^1}{R^2\partial \theta^2} \tag{19}$$
$$M_\theta^1=B_{12}\frac{\partial u^1}{\partial x}+B_{22}\left(\frac{w^1}{R}+\frac{\partial v^1}{R\partial \theta}\right)-D_{22}\frac{\partial^2 w^1}{R^2\partial \theta^2}-D_{12}\frac{\partial^2 w^1}{\partial x^2}$$
$$M_{x\theta}^1=B_{66}\left(\frac{\partial v^1}{\partial x}+\frac{\partial u^1}{R\partial \theta}\right)-D_{66}\frac{\partial^2 w^1}{R\partial x\partial \theta}$$

Substituting Eqs. (18) and (19) into Eqs. (17) gives the stability equations in terms of the displacement components as

$$A_{11}\frac{\partial^2 u^1}{\partial x^2}+A_{66}\frac{\partial^2 u^1}{R^2\partial \theta^2}+(A_{12}+A_{66})\frac{\partial^2 v^1}{R\partial x\partial \theta}+A_{12}\frac{\partial w^1}{R\partial x}-B_{11}\frac{\partial^3 w^1}{\partial x^3}-(B_{12}+B_{66})\frac{\partial^3 w^1}{R^2\partial x\partial \theta^2}=0$$
$$(A_{12}+A_{66})\frac{\partial^2 u^1}{R\partial x\partial \theta}+A_{66}\frac{\partial^2 v^1}{\partial x^2}+A_{22}\frac{\partial^2 v^1}{R^2\partial \theta^2}+A_{22}\frac{\partial w^1}{R^2\partial \theta}-B_{22}\frac{\partial^3 w^1}{R^3\partial \theta^3}-(B_{12}+B_{66})\frac{\partial^3 w^1}{R\partial x^2\partial \theta}=0$$
$$\begin{aligned}B_{11}\frac{\partial^3 u^1}{\partial x^3}+(B_{12}+2B_{66})\frac{\partial^3 u^1}{R^2\partial x\partial \theta^2}-A_{12}\frac{\partial u^1}{R\partial x}+(B_{12}+2B_{66})\frac{\partial^3 v^1}{R\partial x^2\partial \theta}+B_{22}\frac{\partial^3 v^1}{R^3\partial \theta^3}-A_{22}\frac{\partial v^1}{R^2\partial \theta}\\ -D_{11}\frac{\partial^4 w^1}{\partial x^4}-D_{22}\frac{\partial^4 w^1}{R^4\partial \theta^4}+2B_{12}\frac{\partial^2 w^1}{R\partial x^2}+2B_{22}\frac{\partial^2 w^1}{R^3\partial \theta^2}-2(D_{12}+D_{66})\frac{\partial^4 w^1}{R^2\partial x^2\partial \theta^2}\\ -A_{22}\frac{w^1}{R^2}+\bar{N}_x^0\frac{\partial^2 w^1}{\partial x^2}=0\end{aligned} \tag{20}$$

Sandwich cylindrical shells are generally classified by referring to the type of support used in the absent of the body forces and lateral loads except the external temperature load. The boundary conditions are given by

$$\frac{\partial u^1}{\partial x}=v^1=w^1=\frac{\partial^2 w^1}{\partial x^2}=0 \qquad \text{at} \qquad x=0,L \tag{21}$$

The following approximate solution is seen to satisfy both the differential equation and the boundary conditions

$$u^1 = \sum_{m=1}^{\infty}\sum_{n=1}^{\infty} U_{mn}^1 \cos(\lambda x)\sin(\bar{n}\theta)$$
$$v^1 = \sum_{m=1}^{\infty}\sum_{n=1}^{\infty} V_{mn}^1 \sin(\lambda x)\cos(\bar{n}\theta) \quad (22)$$
$$w^1 = \sum_{m=1}^{\infty}\sum_{n=1}^{\infty} W_{mn}^1 \sin(\lambda x)\sin(\bar{n}\theta)$$

$0 \le x \le L,\ 0 \le \theta \le 2\pi$

where $\lambda = m\pi/L$, m and $\bar{n}$ are the number of half-waves in x- and θ-directions, respectively and U_{mn}^1, X_{mn}^1, V_{mn}^1, Y_{mn}^1 and W_{mn}^1 are arbitrary parameters. Substituting Eq. (22) into Eq. (20), one obtains

$$[C]\{\Lambda\} = 0 \quad (23)$$

where $\{\Lambda\}$ denotes the columns

$$\{\Lambda\} = \{U^1\ , V^1\ , W^1\ , X^1\ , Y^1\} \quad (24)$$

The elements c_{ij} of the matrix $[C]$ are given by

$$c_{11} = A_{11}\lambda^2 + A_{66}\left(\frac{\bar{n}}{R}\right)^2 \quad c_{12} = (A_{12} + A_{66})\lambda\frac{\bar{n}}{R} \quad c_{13} = -\frac{A_{12}}{R}\lambda - B_{11}\lambda^3 - (B_{12} + B_{66})\lambda\left(\frac{\bar{n}}{R}\right)^2$$
$$c_{21} = c_{12} \quad c_{22} = A_{66}\lambda^2 + A_{22}\left(\frac{\bar{n}}{R}\right)^2 \quad c_{23} = -A_{22}\frac{\bar{n}}{R^2} - B_{22}\left(\frac{\bar{n}}{R}\right)^3 - (B_{12} + B_{66})\lambda^2\frac{\bar{n}}{R}$$
$$c_{31} = \frac{A_{12}}{R}\lambda + B_{11}\lambda^3 + (B_{12} + 2B_{66})\lambda\left(\frac{\bar{n}}{R}\right)^2 \quad c_{32} = B_{22}\left(\frac{\bar{n}}{R}\right)^3 + A_{22}\frac{\bar{n}}{R^2} + (B_{12} + 2B_{66})\lambda^2\frac{\bar{n}}{R} \quad (25)$$
$$c_{33} = -D11\lambda^4 - 2\frac{B_{12}}{R}\lambda^2 - D_{22}\left(\frac{\bar{n}}{R}\right)^4 - 2B_{22}\frac{\bar{n}^2}{R^3} - 2(D_{12} + D_{66})\lambda^2\left(\frac{\bar{n}}{R}\right)^2 - \frac{A_{22}}{R^2} - \bar{N}_x^0\lambda^2$$

5. Thermal buckling solution

Consider functionally graded sandwich cylindrical shell in which the temperature of the inner and outer surfaces of the cylindrical shell are T_a and T_b, respectively. In the following, the solution of the equation $[C] = 0$ for different types of thermal loading conditions is presented.

5.1 Uniform temperature rise

The cylindrical shell initial temperature is assumed to be T_i. The temperature is uniformly rised to a final value T_f in which the cylindrical shell buckles. The temperature change is

$$\Delta T = T_f - T_i \quad (26)$$

The critical buckling temperature difference is obtained by solving the determinant $|C| = 0$

$$\Delta T_{cr} = \frac{\eta + \mu}{\lambda^2\bar{\beta}_1} \quad (27)$$

where

$$\eta = (c_{11}c_{23}c_{32} - c_{12}c_{23}c_{31} - c_{13}c_{21}c_{32} + c_{13}c_{22}c_{31})/(c_{11}c_{22} - c_{12}c_{21}) \quad (28)$$

$$\mu = D11\lambda^4 + 2\frac{B_{12}}{R}\lambda^2 + D_{22}\left(\frac{\bar{n}}{R}\right)^4 + 2B_{22}\frac{\bar{n}^2}{R^3} + 2(D_{12} + D_{66})\lambda^2\left(\frac{\bar{n}}{R}\right)^2 + \frac{A_{22}}{R^2} \quad (29)$$

$$\bar{\beta}_1 = \sum_{n=1}^{3} \int_{h_{n-1}}^{h_n} \frac{\alpha^{(n)}(z) E^{(n)}(z)}{1-\upsilon} \mathrm{d}z \tag{30}$$

5.2 Linear temperature rise

If the cylindrical shell thickness is thin enough, the temperature distribution is approximated linear through-the-thickness. Therefore, the temperature can be written as

$$T(z) = \Delta T \left(\frac{z}{h} + \frac{1}{2}\right) + T_m \ , \Delta T = T_p - T_m \tag{31}$$

The critical buckling temperature difference can be deduced as

$$\Delta T_{cr} = \frac{\eta + \mu}{\lambda^2 \bar{\beta}_2} - \frac{T_a \bar{\beta}_1}{\bar{\beta}_2} \tag{32}$$

where

$$\bar{\beta}_2 = \sum_{n=1}^{3} \int_{h_{n-1}}^{h_n} \frac{\alpha^{(n)}(z) E^{(n)}(z)}{1-\upsilon} \left(\frac{z}{h} + \frac{1}{2}\right) \mathrm{d}z \tag{33}$$

5.3 Nonlinear temperature rise

The temperature field assumed to be uniform in inner and outer surfaces but varying along the thickness direction due to heat conduction. The temperature distribution can be obtained by solving the steady-state heat transfer equation as:

$$-\frac{d}{dz}\left(K(z)\frac{dT}{dz}\right) = 0 \tag{34}$$

with the boundary conditions $T = T_a$ at $z = -h/2$ and $T = T_b$ at $z = h/2$. The coefficient of thermal conductivity $K(z)$ is assumed to vary continuously through the thickness of the FGM layers according to a sigmoid function or simple power-law distribution in terms of the volume fractions of the constituent. The temperature distribution across the FGM sandwich cylindrical shell thickness is obtained as

$$T(z) = T_a + (T_b - T_a)\Theta^{(n)} \tag{35}$$

where for P-FGM sandwich cylindrical shells

$$\Theta^{(1)} = \frac{\int_{h_0}^{z} \left(1/K^{(1)}(z)\right) dz}{\sum_{n=1}^{3} \int_{h_{n-1}}^{h_n} (1/K^{(n)}(z)) dz}, \qquad h_0 \le z \le h_1 \tag{36}$$

$$\Theta^{(2)} = \frac{\int_{h_0}^{h_1} \left(1/K^{(1)}(z)\right) dz + \int_{h_1}^{z} \left(1/K^{(2)}(z)\right) dz}{\sum_{n=1}^{3} \int_{h_{n-1}}^{h_n} (1/K^{(n)}(z)) dz}, \qquad h_1 \le z \le h_2 \tag{37}$$

$$\Theta^{(3)} = \frac{\int_{h_0}^{h_1}(1/K^{(1)}(z))dz+\int_{h_1}^{h_2}(1/K^{(2)}(z))dz+\int_{h_2}^{z}(1/K^{(3)}(z))dz}{\sum_{n=1}^{3}\int_{h_{n-1}}^{h_n}(1/K^{(n)}(z))dz},\ h_2 \le z \le h_3 \tag{38}$$

and for S-FGM sandwich cylindrical shells

$$\Theta_1^{(1)} = \frac{\int_{h_0}^{z}\left(1/\mathrm{K}_1^{(1)}(z)\right)dz}{\sum_{n=1}^{3}\int_{h_{n-1}}^{h_n}(1/K^{(n)}(z))dz},\ h_0 \le z \le h_m \tag{39}$$

$$\Theta_2^{(1)} = \frac{\int_{h_0}^{h_m}\left(1/\mathrm{K}_1^{(1)}(z)\right)dz+\int_{h_m}^{z}\left(1/\mathrm{K}_2^{(1)}(z)\right)dz}{\sum_{n=1}^{3}\int_{h_{n-1}}^{h_n}(1/K^{(n)}(z))dz}, \qquad h_m \le z \le h_1 \tag{40}$$

$$\Theta^{(2)} = \frac{\int_{h_0}^{h_m}\left(1/\mathrm{K}_1^{(1)}(z)\right)dz + \int_{h_m}^{h_1}\left(1/\mathrm{K}_2^{(1)}(z)\right)dz + \int_{h_1}^{z}(1/K^{(2)}(z))dz}{\sum_{n=1}^{3}\int_{h_{n-1}}^{h_n}(1/K^{(n)}(z))dz}, \qquad h_1 \le z \le h_2 \tag{41}$$

$$\theta_1^{(3)} = \frac{\int_{h_0}^{h_m}\left(1/K_1^{(1)}(z)\right)dz + \int_{h_m}^{h_1}\left(1/K_2^{(1)}(z)\right)dz + \int_{h_1}^{h_2}(1/K^{(2)}(z))dz + \int_{h_2}^{z}\left(1/K_1^{(3)}(z)\right)dz}{\sum_{n=1}^{3}\int_{h_{n-1}}^{h_n}(1/K^{(n)}(z))dz}, \qquad h_2 \le z \le h_n \tag{42}$$

$$\theta_2^{(3)} = \frac{\int_{h_0}^{h_m}\left(1/K_1^{(1)}(z)\right)dz + \int_{h_m}^{h_1}\left(1/K_2^{(1)}(z)\right)dz + \int_{h_1}^{h_2}(1/K^{(2)}(z))dz + \int_{h_2}^{h_n}\left(1/K_1^{(3)}(z)\right)dz + \int_{h_n}^{h_z}\left(1/K_2^{(3)}(z)\right)dz}{\sum_{n=1}^{3}\int_{h_{n-1}}^{h_n}(1/K^{(n)}(z))dz}, \quad h_n \le z \le h_3 \tag{43}$$

where $\Theta^{(n)}$ denotes the nondimensional temperatures change. The critical buckling temperature change under nonlinear temperature rise can be obtain as

$$\Delta T_{cr} = \frac{\eta + \mu}{\lambda^2 \bar{\beta}_3} - \frac{T_a \bar{\beta}_1}{\bar{\beta}_3} \tag{44}$$

where

$$\bar{\beta}_3 = \sum_{n=1}^{3}\int_{h_{n-1}}^{h_n} \frac{\alpha^{(n)}(z)E^{(n)}(z)}{1-\upsilon}\Theta^{(n)}\mathrm{d}z \tag{45}$$

6. Results and discussion

Consider a simply supported FGM sandwich cylindrical shell made of a mixture of metal and ceramic. The combination of materials consists of Steel and Alumina. Young's modulus, coefficient of thermal expansion, and thermal conductivity for Steel are $E_m = 70$ Gpa, $\alpha_m = 23 \times 10^{-6}$ 1/°C, $K_m = 204$ W/mK, , and for Alumina are $E_c = 380$ Gpa, $\alpha_c = 7.4 \times 10^{-6}$ 1/°C, $K_c = 10.4$ W/mK. Poisson's ratio is chosen as constant $\upsilon_c = 0.3$ (Daikh *et al.* 2020). It is assumed that the temperature T_a in the inner surface equal to 25°C. Several kinds of FGM sandwich cylindrical shells are presented:

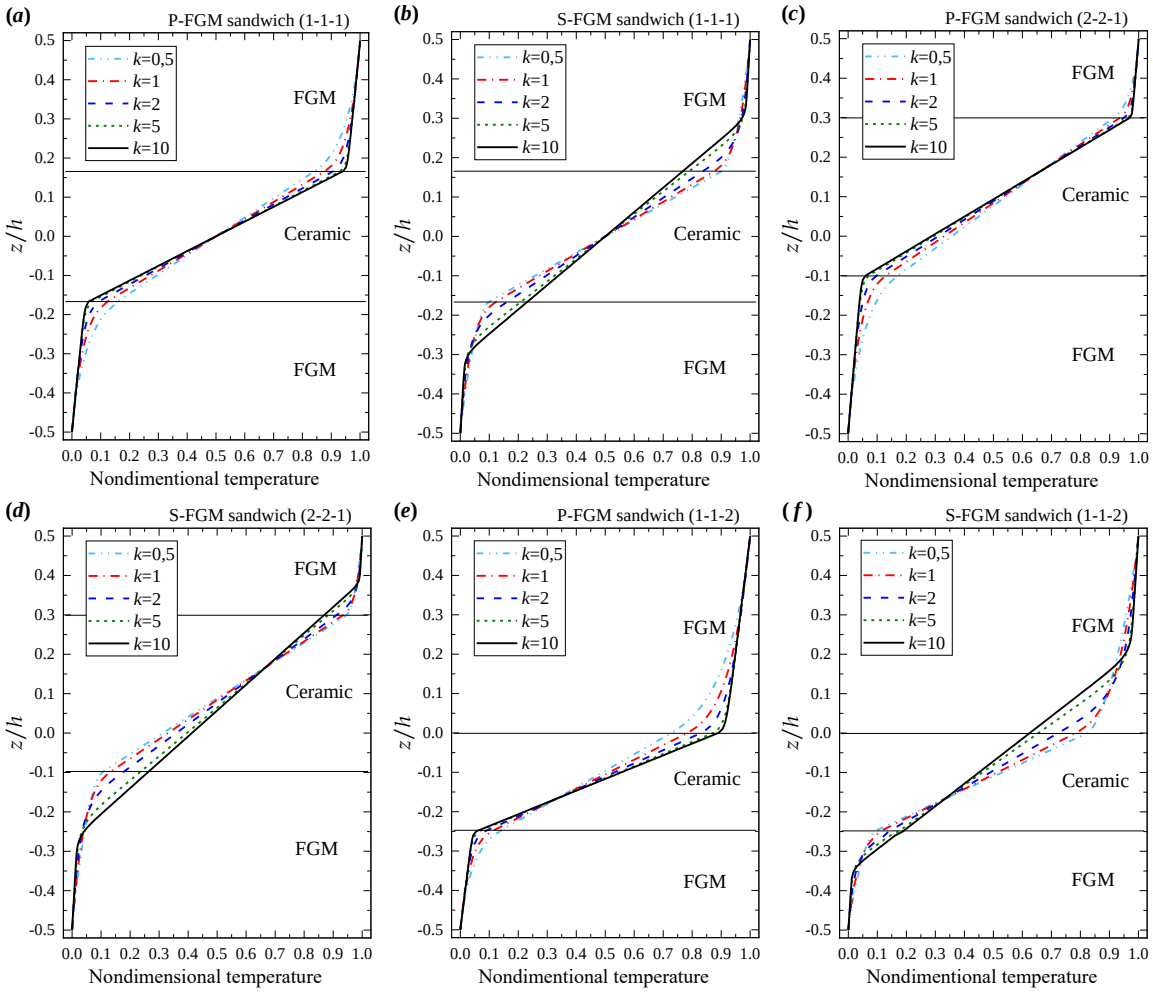

Fig. 3 Nondimensional temperature change across the thickness of FGM sandwich cylindrical shell

The (1–1–1) FGM sandwich cylindrical shell: The shell is made of three equal-thickness layers. In this case, we have:

$$h_1 = -\frac{h}{6},\ h_2 = \frac{h}{6} \tag{46}$$

The (2–2–1) FGM sandwich cylindrical shell: In this case, the core thickness is twice the upper face while it is the same as the lower one. Thus,

$$h_1 = -\frac{h}{10},\ h_2 = \frac{3h}{10} \tag{47}$$

The (1–1–2) FGM sandwich cylindrical shell: The outer layer thickness equals the sum of the two inner layers thickness. In this case, we have:

$$h_1 = -\frac{h}{4}, \qquad h_2 = 0 \tag{48}$$

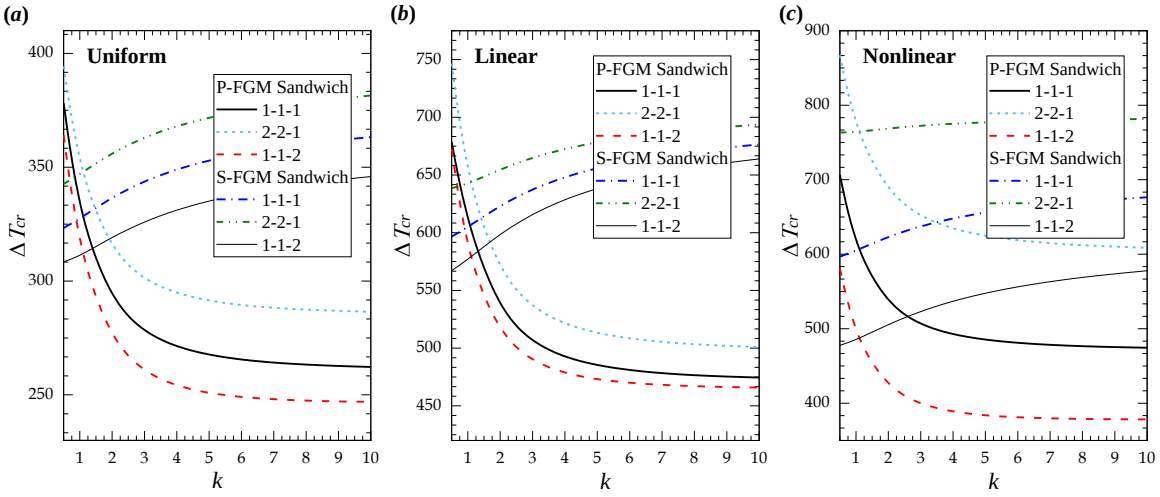

Fig. 4 Critical buckling temperature difference ΔT_{cr} versus the index k (R=L, h=0.01)

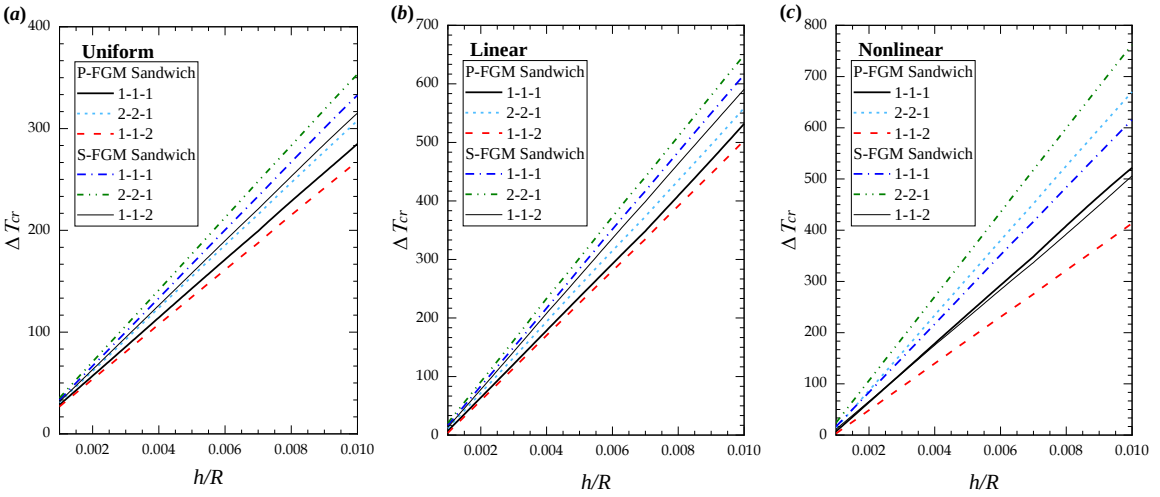

Fig. 5 Critical buckling temperature difference ΔT_{cr} versus the thickness-to-radius ratio h/R (R=L, k=2)

In order to study the nonlinear temperature distribution along the thickness of FGM sandwich cylindrical shells based on the Eqs. (37)-(39) for P-FGM sandwiches and Eqs. (40-44) for S-FGM sandwiches, the nondimensional temperature distribution along the thickness for different values of index k of sandwich shells is presented in Fig. 3. It is seen that, regardless of the sandwich types, the temperature change along the thickness of the homogeneous core is linear, whereas for the FGM face layers it is nonlinear. Because of the low thermal conductivity of ceramic core, the temperature through its thickness decreases rapidly.

The inhomogeneity parameter k has considerable effect on the critical buckling temperature difference of FGM sandwich cylindrical shells as shown in Fig. 4. For the P-FGM sandwich cylindrical shells, it can be observed that with the increase of the parameter k, the critical buckling temperature ΔT_{cr} decreases wherever the thermal loads is, whereas ΔT_{cr} increases for S-FGM sandwich shells. The volume fraction with index k=1 mean that the distribution of material

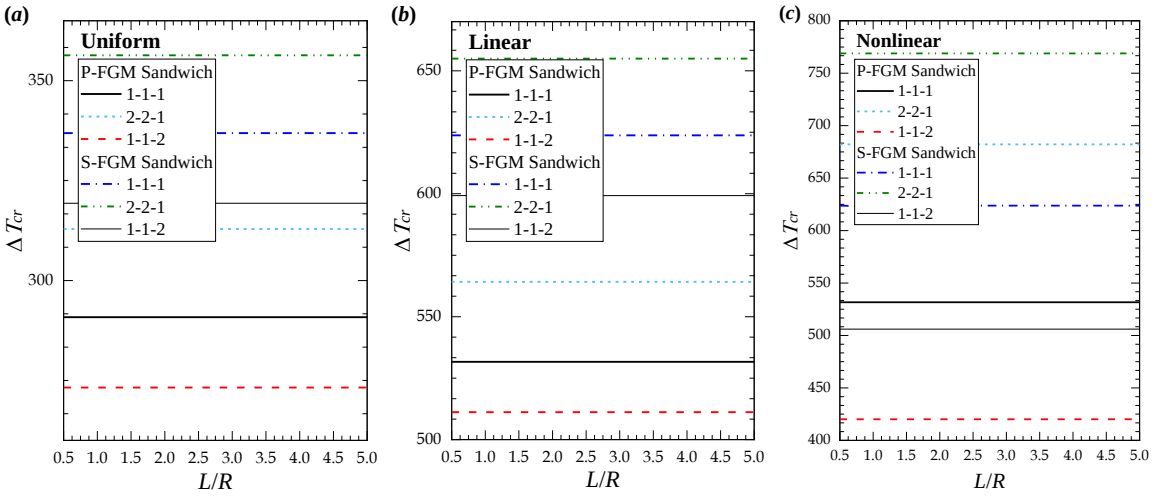

Fig. 6 Critical buckling temperature difference ΔT_{cr} versus the length-to-radius ratio L/R (h=0.01, k=2)

properties is linear through-the-thickness of P-FGM and S-FGM layers, this can explain the same results of critical buckling temperature difference in the sandwiches with same schemes wherever the composition of layer is.

Fig. 5 depicts the effect of shell thickness on the critical buckling temperature difference for various FGM sandwich cylindrical shells. As seen, increasing the thickness-to-radius ratio h/R increases the critical buckling temperature difference. This observation stands for all types FGM sandwiches. Note that the critical buckling temperatures of P-FGM and S-FGM sandwich cylindrical shells with 2-2-1 scheme are noticeably greater than values obtained on other FGM sandwiches.

Fig. 6 shows the variation of critical buckling temperature versus geometric parameter L/R. Critical bucking temperature is almost constant for different values of L/R. From Figs. 5-7, it can be seen that the critical temperatures ΔT_{cr} under uniform temperature rise is smaller than that of the cylindrical shells under linear temperature rise and the latter is smaller than that of the cylindrical shells under nonlinear temperature rise.

7. Conclusions

In this paper, thermal buckling analysis of functionally graded sandwich cylindrical shells has been analyzed. Different schemes of FGM sandwich shells are presented. Material properties of FGM layers are assumed to vary continuously through-the-thickness according to sigmoid function and power-law distribution in terms of the volume fractions of the constituents. The equilibrium and stability equations of FGM sandwich cylindrical shells have been derived based on Donnell theory. Three different thermal loading cases as uniform temperature rise, linear and nonlinear temperature rise through-the-thickness of the cylindrical shell were considered. An exact solution for the critical buckling temperature of FGM sandwich cylindrical shells under nonlinear temperature rise across the thickness is presented. The characteristics of thermal buckling for FGM sandwich cylindrical shells are significantly influenced by volume fraction distributions, system

geometric parameters, and the FGM sandwich Types. The following conclusions are reached:

- The critical buckling temperature difference decreases with increasing of the volume fraction index k for P-FGM sandwiches and increase for S-FGM sandwiches.
- The critical buckling temperature difference increases linearly with the increasing of the thickness-to-radius ratio h/R for all types and schemes of FGM sandwiches wherever the thermal load type is.
- The critical buckling temperature difference is almost constant for different values of L/R.

The critical temperatures ΔT_{cr} of cylindrical shells under uniform temperature rise is smaller than that of the cylindrical shells under linear temperature rise and the latter is smaller than that of the cylindrical shells under nonlinear temperature rise.

Acknoweledgments

This research was supported by the Algerian Directorate General of Scientific Research and Technological Development (DGRSDT) and University of Mustapha Stambouli of Mascara (UMS Mascara) in Algeria.

References

Asadi, H., Akbarzadeh, A.H., Chen, Z.T. and Aghdam, M.M. (2015), "Enhanced thermal stability of functionally graded sandwich cylindrical shells by shape memory alloys", *Smart Mater. Struct.*, **24**(4), 045022. http://doi.org/10.1088/0964-1726/24/4/045022.

Bagherizadeh, E., Kiani, Y. and Eslami, M.R. (2012), "Thermal buckling of functionally graded material cylindrical shells on elastic foundation", *AIAA J.*, **50**(2), 500-503. https://doi.org/10.2514/1.J051120.

Brush D.O. and Almroth, B.O. (1975), *Buckling of Bars, Plates and Shells*, McGraw-Hill, New York, U.S.A.

Daikh, A.A. and Zenkour, A.M. (2019a), "Effect of porosity on the bending analysis of various functionally graded sandwich plates", *Mater. Res. Express*, **6**, 065703. https://doi.org/10.1088/2053-1591/ab0971.

Daikh, A.A. and Zenkour, A.M. (2019b), "Free vibration and buckling of porous power-law and sigmoid functionally graded sandwich plates using a simple higher-order shear deformation theory", *Mater. Res. Express*, **6**, 115707. https://doi.org/10.1088/2053-1591/ab48a9.

Daikh, A.A., Guerroudj, M., Elajrami M. and Megueni, A. (2020), "Thermal buckling of functionally graded sandwich beams", *Adv. Mater. Res.*, **1156**, 43-59. https://doi.org/10.4028/www.scientific.net/AMR.1156.43.

Dung, D.V. and Nga, N.T. (2013), "Nonlinear buckling and postbuckling of eccentrically stiffened functionally graded cylindrical shells surrounded by and elastic medium based on the first order shear deformation theory", *Vietnam J. Mech.*, **35**, 285-298. https://doi.org/10.15625/0866-7136/35/4/3116.

Finot, M., Suresh, S., Bull, C. and Sampath., S. (1996), "Curvature changes during thermal cycling of a compositionally graded Ni/$A1_2O_3$ multi-layered material", *Mater. Sci. Eng. A*, **205**, 59-71. https://doi.org/10.1016/0921-5093(95)09892-5.

Han, Q., Wang, Z., Nash, D.H. and Liu, P. (2017), "Thermal buckling analysis of cylindrical shell with functionally graded material coating", *Compos. Struct.*, **181**, 171-182. http://doi.org/10.1016/j.compstruct.2017.08.085.

Hoang, V.T. and Nguyen., D.D. (2008), "Thermal buckling of imperfect functionally graded cylindrical shells According to Wan-Donnell model", *Vietnam J. Mech.*, **30**(3), 185-194. https://doi.org/10.15625/0866-7136/30/3/5618.

Huang, H., Han, Q. and Wei, D. (2011), "Buckling of FGM cylindrical shells subjected to pure bending load", *Compos. Struct.*, **93**, 2945-2952. https://doi.org/10.1016/j.compstruct.2011.05.009.

Kadoli, R. and Ganesan, N. (2006), "Buckling and free vibration analysis of functionally graded cylindrical

shells subjected to a temperature-specified boundary condition", *J. Sound Vib.*, **289**, 450-480. https://doi.org/10.1016/j.jsv.2005.02.034.

Kar, V.R., Panda, S.K. and Mahapatra, T.R. (2016), "Thermal buckling behaviour of shear deformable functionally graded single/doubly curved shell panel with TD and TID properties", *Adv. Mater. Res.*, **5**(4), 205-221. https://doi.org/10.12989/amr.2016.5.4.205.

Lang, Z. and Xuewu, L. (2013), "Buckling and vibration analysis of functionally graded magneto-electro-thermo-elastic circular cylindrical shells", *Appl. Math. Model.*, **37**, 2279-2292. http://doi.org/10.1016/j.apm.2012.05.023.

Lang, Z. and Xuewu, L. (2013), "Buckling and vibration analysis of functionally graded magneto-electro-thermo-elastic circular cylindrical shells", *Appl. Math. Model.*, **37**(4), 2279-2292. https://doi.org/10.1016/j.apm.2012.05.023.

Mehralian, F., Beni, Y.T. and Ansari, R. (2016), "Size dependent buckling analysis of functionally graded piezoelectric cylindrical nanoshell", *Compos. Struct.*, **152**, 45-61. https://doi.org/10.1016/j.compstruct.2016.05.024.

Mirzavand, B. and Eslami, M.R. (2006), "Thermal buckling of imperfect functionally graded cylindrical shells based on the Wan-Donnell model", *J. Therm. Stresses*, **29**(1), 37-55. https://doi.org/10.1080/01495730500257409.

Mirzavand, B. and Eslami, M.R. (2007), "Thermal buckling of simply supported piezoelectric FGM cylindrical shells", *J. Therm. Stresses*, **30**(11), 1117-1135. https://doi.org/10.1080/01495730701416036.

Mirzavand, B., Eslami, M.R. and Shahsiah, R. (2005), "Effect of imperfections on thermal buckling of functionally graded cylindrical shells", *AIAA J.*, **43**(9), 2073-2076. https://doi.org/10.2514/1.12900.

Miyamoto, Y., Kaysser, W.A., Rabin, B.H., Kawasaki, A. and Ford, R.G. (1999), *Functionally Graded Materials: Design, Processing and Applications*, Kluwer Academic, Boston, U.S.A.

Najafizadeh, M.M, Hasani, A. and Khazaeinejad, P. (2009), "Mechanical stability of functionally graded stiffened cylindrical shells", *Appl. Math. Model.*, **33**, 1151-1157. https://doi.org/10.1016/j.apm.2008.01.009.

Nasirmanesh, A. and Mohammadi, S. (2016), "Eigenvalue buckling analysis of cracked functionally graded cylindrical shells in the framework of the extended finite element method", *Compos. Struct.*, **159**, 548-566. https://doi.org/10.1016/j.compstruct.2016.09.065.

Ni, Y., Tong, Z., Rong, D., Zhou, Z. and Xu, X. (2018), "Accurate thermal buckling analysis of functionally graded orthotropic cylindrical shells under the symplectic framework", *Thin-Walled Struct.*, **129**, 1-9. https://doi.org/10.1016/j.tws.2018.03.030.

Ni, Y.W., Tong, Z.Z., Rong, D.L., Zhou, Z.H. and Xu, X.S. (2017), "A new Hamiltonian-based approach for free vibration of a functionally graded orthotropic circular cylindrical shell embedded in an elastic medium", *Thin-Walled Struct.*, **120**, 236-248. http://doi.org/10.1016/j.tws.2017.09.003.

Sabzikar Boroujerdy, M., Naj, R. and Kiani, Y. (2014), "Buckling of heated temperature dependent FGM cylindrical shell surrounded by elastic medium", *J. Theor. Appl. Mech.*, **52**(4), 869-881. https://doi.org/10.15632/jtam-pl.52.4.869.

Shahsiah, R. and Eslami, M.R. (2003a), "Functionally graded cylindrical shell thermal instability based on improved Donnell equations", *AIAA J.*, **41**(9), 1819-1826. https://doi.org/10.2514/2.7301.

Shahsiah, R. and Eslami, M.R. (2003b) "Thermal buckling of functionally graded cylindrical shells", *J. Therm. Stresses*, **26**, 277-294. https://doi.org/10.1080/713855892.

Shariyat, M. and Asgari, D. (2013), "Nonlinear thermal buckling and postbuckling analyses of imperfect variable thickness temperature-dependent bidirectional functionally graded cylindrical shells", *Int. J. Pressure Vessels Piping*, **112**, 310-320. http://doi.org/10.1016/j.ijpvp.2013.09.005.

Shaterzadeh, A. and Foroutan, K. (2016), "Post-buckling of cylindrical shells with spiral stiffeners under elastic foundation", *Struct. Eng. Mech.*, **60**(4), 615-631. http://doi.org/10.12989/sem.2016.60.4.615.

Sheng, G.G. and Wang, X. (2008), "Thermal vibration, buckling and dynamic stability of functionally graded cylindrical shells embedded in an elastic medium", *J. Reinf. Plast. Compos.*, **27**(2), 117-134. https://doi.org/10.1177/0731684407082627.

Sheng, G.G. and Wang, X. (2008), "Thermal vibration, buckling and dynamic stability of functionally

graded cylindrical shells embedded in an elastic medium", *J. Reinf. Plast. Compos.*, **27**(2), 117-134. https://doi.org/10.1177/0731684407082627.

Sheng, G.G. and Wang, X. (2010), "Thermoelastic vibration and buckling analysis of functionally graded piezoelectric cylindrical shells", *Appl. Math. Model.*, **34**, 2630-2643. https://doi.org/10.1016/j.apm.2009.11.024.

Sofiyev A.H. (2014), "The vibration and buckling of sandwich cylindrical shells covered by different coatings subjected to the hydrostatic pressure", *Compos. Struct.*, **117**, 124-134. http://doi.org/10.1016/j.compstruct.2014.06.025.

Sun, J., Lim, C.W., Zhou, Z., Xu, X. and Sun, W. (2016), "Rigorous buckling analysis of size-dependent functionally graded cylindrical nanoshells", *J. Appl. Phys.*, **119**, 214303. https://doi.org/10.1063/1.4952984.

Thang, P.T., Duc, N.D. and Nguyen-Thoi, T. (2016), "Effects of variable thickness and imperfection on nonlinear buckling of sigmoidfunctionally graded cylindrical panels", *Compos. Struct.*, **155**, 99-106. http://doi.org/10.1016/j.compstruct.2016.08.007.

Thang, P.T., Duc, N.D. and Nguyen-Thoi, T. (2017), "Thermomechanical buckling and post-buckling of cylindrical shell with functionally graded coatings and reinforced by stringers", *Aerosp. Sci. Technol.*, **66**, 392-401. http://doi.org/10.1016/j.ast.2017.03.023

Thangaratnam, R.K., Palaninathan, R. and Ramachandran, J. (1990), "Thermal buckling of laminated composite shells", *AIAA J.*, **28**(5), 859-860. http://doi.org/10.2414/3.25130.

Trabelsi, S., Frikha, A., Zghal, S. and Dammak, F. (2019), "A modified FSDT-based four nodes finite shell element for thermal buckling analysis of functionally graded plates and cylindrical shells", *Eng. Struct.*, **178**, 444-459. https://doi.org/10.1016/j.engstruct.2018.10.047.

Wan, Z. and Li, S. (2017), "Thermal buckling analysis of functionally graded cylindrical shells", *Appl. Math. Mech.*, **38**(8), 1059-1070. https://doi.org/10.1007/s10483-017-2225-7.

Wu, L., Jiang, Z. and Liu, J. (2005), "Thermoelastic stability of functionally graded cylindrical shells", *Compos. Struct.*, **70**, 60-68. https://doi.org/10.1016/j.compstruct.2004.08.012.

Zenkour, A.M. and Sobhy, M. (2010), "Thermal buckling of various types of FGM sandwich plates", *Compos. Struct.*, **93**(1), 93-102. https://doi.org/10.1016/j.compstruct.2010.06.012.

Zhang, Y., Huang, H. and Han, Q. (2015), "Buckling of elastoplastic functionally graded cylindrical shells under combined compression and pressure", *Compos. Part B*, **69**, 120-126. http://doi.org/10.1016/j.compositesb.2014.09.024.

Zhou, Z.H., Ni, Y.W., Tong, Z.Z., Zhu, S.B., Sun, J.B. and Xu, X.S. (2019a), "Accurate nonlinear buckling analysis of functionally graded porous graphene platelet reinforced composite cylindrical shells", *Int. J. Mech. Sci.*, **151**, 537-550. https://doi.org/10.1016/j.ijmecsci.2018.12.012.

Zhou, Z.H., Ni, Y.W., Tong, Z.Z., Zhu, S.B., Sun, J.B. and Xu, X.S. (2019b), "Accurate nonlinear stability analysis of functionally graded multilayer hybrid composite cylindrical shells subjected to combined loads", *Mater. Des.*, **182**, 108035. https://doi.org/10.1016/j.matdes.2019.108035.

CC